intrinsic light scattering in bR) will help establish the exact nature of the field interaction. The main conclusion is that the experiment is clearly in the weak field limit and the laser field is not strongly perturbing the underlying thermally populated modes, but rather inducing their interference in the excited-state surface. Isomerization yields were also compared with and without phase control (Fig. 6C), keeping spectral amplitudes constant (Fig. 6D; spectral profiles were confirmed using a tunable monochromator with 0.2-nm spectral resolution). The data show a clear phase dependence indicative of coherent control.

Pure amplitude modulation alters the temporal profile of the pulse (fig. S5); therefore, removing the phase modulation affects the isomerization yield by only 5 to 7%. The phase sensitivity of the control efficiency further illustrates the coherent nature of the state preparation.

The temporal profiles of the shaped optimal and anti-optimal pulses and the observed degree of the isomerization yield control are consistent with the known fast electronic dephasing of bR (10, 38). The largest field amplitudes are confined to approximately 300-fs widths to yield 20% control. In the case of transform-limited pulses, all the vibrational levels within the excitation bandwidth are excited in phase and there is a fast decoherence in the initial electronic polarization (38). However, with the phase-selective restricted bandwidths in the shaped pulses, there is an opportunity to manipulate different vibrational states with much longer coherence times than the electronic polarization. The resultant constructive and destructive interference effects involving vibrational modes displaced along the reaction coordinate offer the possibility of controlling isomerization. Experimental observations presented here show that the wave properties of matter can play a role in biological processes, to the point that they can even be manipulated.

References and Notes

1. M. Shapiro, P. Brumer, *Rep. Prog. Phys.* **66**, 859 (2003).
2. S. H. Shi, H. Rabitz, *J. Chem. Phys.* **92**, 364 (1990).
3. W. T. Pollard, S. Y. Lee, R. A. Mathies, *J. Chem. Phys.* **92**, 4012 (1990).
4. Q. Wang, R. W. Schoenlein, L. A. Peteanu, R. A. Mathies, C. V. Shank, *Science* **266**, 422 (1994).
5. K. C. Hasson, F. Gai, P. A. Anfinrud, *Proc. Natl. Acad. Sci. U.S.A.* **93**, 15124 (1996).
6. T. Ye *et al.*, *J. Phys. Chem. B* **103**, 5122 (1999).
7. R. Gonzalez-Luque *et al.*, *Proc. Natl. Acad. Sci. U.S.A.* **97**, 9379 (2000).
8. T. Kobayashi, T. Saito, H. Ohtani, *Nature* **414**, 531 (2001).
9. J. Herbst, K. Heyne, R. Diller, *Science* **297**, 822 (2002).
10. J. T. M. Kennis *et al.*, *J. Phys. Chem. B* **106**, 6067 (2002).
11. S. Hayashi, E. Tajkhorshid, K. Schulten, *Biophys. J.* **85**, 1440 (2003).
12. S. C. Flores, V. S. Batista, *J. Phys. Chem. B* **108**, 6745 (2004).
13. Y. Ohtsuki, K. Ohara, M. Abe, K. Nakagami, Y. Fujimura, *Chem. Phys. Lett.* **369**, 525 (2003).
14. G. Vogt, G. Krampert, P. Niklaus, P. Nuernberger, G. Gerber, *Phys. Rev. Lett.* **94**, 068305 (2005).
15. K. Hoki, P. Brumer, *Phys. Rev. Lett.* **95**, 168305 (2005).
16. J. L. Herek, W. Wohlleben, R. J. Cogdell, D. Zeidler, M. Motzkus, *Nature* **417**, 533 (2002).
17. J. Tittor, D. Oesterhelt, *FEBS Lett.* **263**, 269 (1990).
18. S. L. Logunov, M. A. El-Sayed, *J. Phys. Chem. B* **101**, 6629 (1997).
19. H. J. Polland *et al.*, *Biophys. J.* **49**, 651 (1986).
20. F. Gai, K. C. Hasson, J. C. McDonald, P. A. Anfinrud, *Science* **279**, 1886 (1998).
21. See supporting data on *Science* Online.
22. V. I. Prokhorenko, A. M. Nagy, R. J. D. Miller, *J. Chem. Phys.* **122**, 184502 (2005).
23. A. K. Dioumaev, V. V. Savransky, N. V. Tkachenko, V. I. Chukharev, *J. Photochem. Photobiol. B Biol.* **3**, 397 (1989).
24. G. Schneider, R. Diller, M. Stockburger, *Chem. Phys.* **131**, 17 (1989).
25. A. Xie, *Biophys. J.* **58**, 1127 (1990).
26. S. P. Balashov, E. S. Imasheva, R. Govindjee, T. G. Ebrey, *Photochem. Photobiol.* **54**, 955 (1991).
27. J. Paye, *IEEE J. Quant. Electron.* **28**, 2262 (1992).
28. H. L. Fragnito, J.-Y. Bigot, P. C. Becker, C. V. Shank, *Chem. Phys. Lett.* **160**, 101 (1989).
29. A. B. Myers, R. A. Harris, R. A. Mathies, *J. Chem. Phys.* **79**, 603 (1983).
30. B. X. Hou, N. Friedman, M. Ottolenghi, M. Sheves, S. Ruhman, *Chem. Phys. Lett.* **381**, 549 (2003).
31. R. Morita, M. Yamashita, A. Suguro, H. Shigekawa, *Opt. Commun.* **197**, 73 (2001).
32. K. Blum, *Density Matrix Theory and Applications* (Plenum, New York, 1981).
33. D. Gelman, R. Kosloff, *J. Chem. Phys.* **123**, 234506 (2005).
34. J. Hauer, H. Skenderovic, K.-L. Kompa, M. Motzkus, *Chem. Phys. Lett.* **421**, 523 (2006).
35. D. Oesterhelt, W. Stoeckenius, in *Methods in Enzymology*, vol. 31 of *Biomembranes* (Academic Press, New York, 1974), pp. 667–678.
36. The saturation energy is related to the absorption cross section σ as $E_s = 1/\sigma_{trans}$ (for a negligibly small contribution of the excited-state emission), and σ is related to the extinction coefficient ε as $\sigma = [\log(10)/N_A]\varepsilon = 3.86 \times 10^{-21}\varepsilon$, where N_A is Avogadro's number.
37. The fraction of excited molecules can be estimated as a ratio between the number of absorbed photons $n_p = E_{exc} \times \pi d_0^2/4$ and the number of retinal molecules $N_m = C \times V$ in an excited volume $V_0 \cong l_0 \times \pi d_0^2/4$, where the concentration is $C = 2.303 A_0/\sigma_{trans}$, A_0 is OD at 565 nm (0.9), $l_0 = 0.04$ cm is the path length in the cell used, and $d_0 = 0.015$ cm is the beam diameter in the sample. This gives a fraction of excited molecules of 0.0236 (that is, 1 out of 42.3 molecules will be excited during the excitation pulse at a given fluence). The fraction of double-excited molecules can be estimated from the Poisson distribution $f(k) = e^{-\lambda}(\lambda)^k/k!$, where λ = 0.0236, and k is the number of occurrences ($k = 1$ for the single excitation, $k = 2$ for the double excitation, etc.). Thus, the fraction of double-excited molecules $f(2)/f(1) = \lambda/2$; that is, 1.18%.
38. V. F. Kamalov, T. M. Masciangioli, M. A. El-Sayed, *J. Phys. Chem.* **100**, 2762 (1996).
39. K. Edman *et al.*, *Nature* **401**, 822 (1999).
40. This work was supported by the National Sciences and Engineering Research Council of Canada. The authors thank J.T.M. Kennis, Vrije Universiteit Amsterdam, for helpful discussions of preliminary results.

Phytophthora Genome Sequences Uncover Evolutionary Origins and Mechanisms of Pathogenesis

Brett M. Tyler,[1]* Sucheta Tripathy,[1] Xuemin Zhang,[1] Paramvir Dehal,[2,3] Rays H. Y. Jiang,[1,4] Andrea Aerts,[2,3] Felipe D. Arredondo,[1] Laura Baxter,[5] Douda Bensasson,[2,3,6] Jim L. Beynon,[5] Jarrod Chapman,[2,3,7] Cynthia M. B. Damasceno,[8] Anne E. Dorrance,[9] Daolong Dou,[1] Allan W. Dickerman,[1] Inna L. Dubchak,[2,3] Matteo Garbelotto,[10] Mark Gijzen,[11] Stuart G. Gordon,[9] Francine Govers,[4] Niklaus J. Grunwald,[12] Wayne Huang,[2,14] Kelly L. Ivors,[10,15] Richard W. Jones,[16] Sophien Kamoun,[9] Konstantinos Krampis,[1] Kurt H. Lamour,[17] Mi-Kyung Lee,[18] W. Hayes McDonald,[19] Mónica Medina,[20] Harold J. G. Meijer,[4] Eric K. Nordberg,[1] Donald J. Maclean,[21] Manuel D. Ospina-Giraldo,[22] Paul F. Morris,[23] Vipaporn Phuntumart,[23] Nicholas H. Putnam,[2,3] Sam Rash,[2,13] Jocelyn K. C. Rose,[24] Yasuko Sakihama,[25] Asaf A. Salamov,[2,3] Alon Savidor,[17] Chantel F. Scheuring,[18] Brian M. Smith,[1] Bruno W. S. Sobral,[1] Astrid Terry,[2,13] Trudy A. Torto-Alalibo,[1] Joe Win,[9] Zhanyou Xu,[18] Hongbin Zhang,[18] Igor V. Grigoriev,[2,3] Daniel S. Rokhsar,[2,7] Jeffrey L. Boore[2,3,26,27]

Draft genome sequences have been determined for the soybean pathogen *Phytophthora sojae* and the sudden oak death pathogen *Phytophthora ramorum*. Oömycetes such as these *Phytophthora* species share the kingdom Stramenopila with photosynthetic algae such as diatoms, and the presence of many *Phytophthora* genes of probable phototroph origin supports a photosynthetic ancestry for the stramenopiles. Comparison of the two species' genomes reveals a rapid expansion and diversification of many protein families associated with plant infection such as hydrolases, ABC transporters, protein toxins, proteinase inhibitors, and, in particular, a superfamily of 700 proteins with similarity to known oömycete avirulence genes.

*P*hytophthora plant pathogens attack a wide range of agriculturally and ornamentally important plants (1). Late blight of potato caused by *Phytophthora infestans* resulted in the Irish potato famine in the 19th cen-

tury, and *P. sojae* costs the soybean industry millions of dollars each year. In California and Oregon, a newly emerged *Phytophthora* species, *P. ramorum*, is responsible for a disease called sudden oak death (2) that affects not only the live

oaks that are the keystone species of the ecosystem but also a large variety of woody shrubs that inhabit the oak ecosystems, such as bay laurel and viburnum (2). Many other members of the oömycete phylum are plant or animal pathogens, and some pose biosecurity threats such as the maize downy mildews *Peronosclerospora philippinesis* and *Sclerophthora rayssiae*. Extensive classical and molecular genetic tools and genomics resources have been developed for *P. sojae* and *P. infestans* (3, 4).

Oömycetes fall within the kingdom Stramenopila (5, 6), which also includes golden-brown algae, diatoms, and brown algae such as kelp (Fig. 1A). The algal stramenopiles are secondarily photosynthetic, having engulfed a red alga and adopted its plastid approximately 1,300 million years ago (6). However, nonphotosynthetic stramenopiles, such as the oömycetes, do not even have the vestigial plastids found in apicomplexan and euglenoid parasites that originate from phototrophs. Therefore, an important evolutionary question is whether the kingdom Stramenopila was founded by a photosynthetic or nonphotosynthetic organism and, more generally, whether a much larger group of secondarily photosynthetic organisms, called the

[1]Virginia Bioinformatics Institute, Virginia Polytechnic Institute and State University, Blacksburg, VA 24061, USA. [2]Department of Energy Joint Genome Institute, Walnut Creek, CA 94598, USA. [3]Genomics Division, Ernest Orlando Lawrence Berkeley National Laboratory, Berkeley, CA 94720, USA. [4]Laboratory of Phytopathology, Wageningen University, NL-6709 PD Wageningen, Netherlands. [5]Horticulture Research International, Wellesbourne, Warwick CV35 9EF, United Kingdom. [6]Department of Biological Sciences, Imperial College, London SL5 7PY, United Kingdom. [7]Center for Integrative Genomics, University of California, Berkeley, CA 94720, USA. [8]Department of Plant Pathology, Cornell University, Ithaca, NY 14853, USA. [9]Department of Plant Pathology, Ohio Agricultural Research and Development Center, The Ohio State University, Wooster, OH 44691, USA. [10]Department of Environmental Science, Policy, and Management, Ecosystem Sciences Division, University of California, Berkeley, CA 94720, USA. [11]Agriculture and Agri-Food Canada, London, ON, Canada, N5V 4T3. [12]Horticultural Crops Research Laboratory, USDA Agricultural Research Service, Corvallis, OR 97330, USA. [13]Biosciences Directorate, [14]Computation Directorate, Lawrence Livermore National Laboratory, Livermore, CA 94550, USA. [15]North Carolina State University Mountain Horticultural Crops Research and Extension Center, Fletcher, NC 28732, USA. [16]Vegetable Laboratory, Henry Wallace Beltsville Agriculture Research Center, USDA Agricultural Research Service, Beltsville, MD 20705, USA. [17]Department of Entomology and Plant Pathology, University of Tennessee, Knoxville, TN 37996, USA. [18]Department of Soil and Crop Sciences, Texas A&M University, College Station, TX 77843, USA. [19]Chemical Sciences Division, Oak Ridge National Laboratory, Oak Ridge, TN 37831, USA. [20]School of Natural Sciences, University of California, Merced, CA 95344, USA. [21]Department of Biochemistry & Molecular Biology, University of Queensland, St. Lucia, Queensland 4072, Australia. [22]Department of Biology, Wilkes University, Wilkes-Barre, PA 18766, USA. [23]Department of Biological Sciences, Bowling Green State University, Bowling Green, OH 43402, USA. [24]Department of Plant Biology, Cornell University, Ithaca, NY 14853, USA. [25]Laboratory of Ecological Chemistry, Hokkaido University, Sapporo 060-8589, Japan. [26]Department of Integrative Biology, University of California, Berkeley, CA 94720, USA. [27]Genome Project Solutions, Hercules, CA 94547, USA.

*To whom correspondence should be addressed. E-mail: bmtyler@vt.edu

chromalveolates (6), was founded by a single photosynthetic ancestor.

We report here the draft genome sequences of *P. sojae* and *P. ramorum*. The sequences, a nine-fold coverage of the 95 Mb *P. sojae* genome and a seven-fold coverage of the 65 Mb *P. ramorum* genome, were produced using a whole-genome shotgun approach (7). We constructed a physical map of *P. sojae* to aid the sequence assembly by using restriction enzyme fingerprinting of bacterial artificial chromosome (BAC) clones from two libraries (7). We identified 19,027 predicted genes (gene models) in the genome of *P. sojae* and 15,743 in the genome of *P. ramorum*, supported in part by expressed sequence tags (ESTs) from *P. sojae* and proteomic surveys in *P. ramorum* (7). Of these, 9768 pairs of gene models could be identified as putative orthologs (7). There are 1755 gene models in *P. sojae* and 624 in *P. ramorum* encoding unique proteins that do not have a homolog in the other genome at a significance threshold of 10^{-8}. The overall higher number of predicted genes in *P. sojae* results from a greater size of many gene families within the species.

There is extensive colinearity of orthologs between the two genomes. One colinear block, illustrated in Fig. 2, spans 1.8 Mb of *P. sojae* sequence and 0.8 Mb of *P. ramorum* sequence and contains 425 *P. sojae* and 265 *P. ramorum* genes, respectively, of which 170 are orthologous (7). The longest colinear block spans an estimated 4.8 Mb in *P. sojae* and 2.9 Mb in *P. ramorum* and contains 1129 *P. sojae* and 793 *P. ramorum* gene models, respectively, of which 463 are orthologous. The long-range colinearity between the two genomes is preserved despite the presence of many local rearrangements and many nonorthologous genes. Local disruptions of the gene colinearity are particularly common in the vicinity of genes associated with plant infection such as *P. sojae Avr1b*-1 (8) (Fig. 2B).

The genome sequences of *P. sojae* and *P. ramorum* imply several metabolic idiosyncrasies. For example, the CYP51 group of cytochrome P450 enzymes are considered necessary for sterol biosynthesis (9). Consistent with *Phytophthora* being sterol auxotrophs, none of these genes could be identified in either *Phytophthora* genome, although most other sterol biosynthetic genes could be recognized. More unexpectedly, neither genome appears to contain any gene for phospholipase C (PLC), an enzyme present in all eukaryotes sequenced so far (10), nor are PLC sequences present in a collection of 75,757 ESTs from *Phytophthora infestans* (11). In contrast, the diatom *Thalassiosira pseudonana* has three PLC genes. No other highly conserved genes were identified as missing from both the *P. sojae* and *P. ramorum* genomes.

Because *P. ramorum* has recently appeared in California and Europe, an important priority is the development of genetic markers for population genetics and strain tracking of the

pathogen. Through sequencing the *P. ramorum* genome, we identified ~13,643 single nucleotide polymorphisms (SNPs) (7) and numerous simple sequence repeats useful for this purpose. The *P. sojae* genome sequence contains only 499 SNPs, probably because *P. sojae* is homothallic (inbreeding), whereas *P. ramorum* is heterothallic (outcrossing).

To address whether the kingdom Stramenopila might have been founded by a photosynthetic ancestor (6), we searched for *Phytophthora* genes that had especially strong similarities to genes of photosynthetic organisms (7). We identified 855 genes with a putative heritage from a red alga or cyanobacterium (fig. S2), of which 30 are detailed in table S4. Some of the most striking examples of the putative acquisition of genes from a photosynthetic ancestor are provided by genes encoding biosynthetic enzymes targeted to the chloroplasts of photosynthetic organisms and to the mitochondria of nonphotosynthetic organisms. Table S4 includes 12 genes whose protein product has a predicted mitochondrial location in *Phytophthora* and a predicted plastid location in plants and/or algae. One example, the gene for 2-isopropylmalate synthase (functioning in leucine biosynthesis), is shown in Fig. 1B. Although a few details of this tree appear to be anomalous, owing perhaps to the ancient separation of these lineages and sparse taxon sampling, there are clearly two major phylogenetic groups of this gene: one acquired in fungi by transfer from an α-proteobacterium, presumably the endosymbiont that gave rise to mitochondria, and the other acquired in algae, plants, and stramenopiles from a cyanobacterium, presumably the endosymbiont that originally gave rise to plastids. It is further interesting that this gene in the diatom *Thalassiosira pseudonana* groups with those of green plants rather than red algae, perhaps indicating a separate ancestry, as has been suggested for some other chromalveolates (12, 13), although this could alternatively be an artifact due to incomplete sampling of lineages or of the genes within them. Figure 1C shows a more unusual example, from the sixth step of purine biosynthesis. The two *Phytophthora* species, together with the diatom *Thalassiosira pseudonana* and the green alga *Chlamydomonas reinhardtii*, are unique among eukaryotes because they have a prokaryotic, organelle-targeted N-phosphoribosyl-carboxy-aminoimidazole (NCAIR) mutase homolog closely resembling that of cyanobacteria (14), in addition to a conventional eukaryotic, cytoplasmic-targeted 1-(5-phosphoribosyl)-5-amino-4-imidazole (AIR) carboxylase (Fig. 1C). The presence of numerous genes of putative phototroph origin in the *Phytophthora* genomes lends support to the hypothesis that the stramenopile ancestor was photosynthetic, which is consistent with the chromalveolate hypothesis.

Genes involved in the interactions of *P. sojae* and *P. ramorum* with their hosts are of central interest. Motile *Phytophthora* zoospores exhibit

chemotaxis toward signals from host tissue such as isoflavones (*15*). In other eukaryotes, chemotaxis reception is mediated by G protein–coupled receptors (GPCRs) (*16*). *P. sojae* and *P. ramorum* each have 24 GPCRs, four of which show a top match to the *Dictyostelium* cyclic adenosine monophosphate chemotaxis receptor. Another 12 GPCRs have a C-terminal intracellular phosphatidylinositol-4-phosphate 5-kinase domain similar to the RpkA gene of *Dictyostelium* (*17*); this domain would enable signaling to bypass the heterotrimeric G proteins, perhaps explaining why the *Phytophthora* genomes contain only single genes for G-α and G-β subunits (*17*).
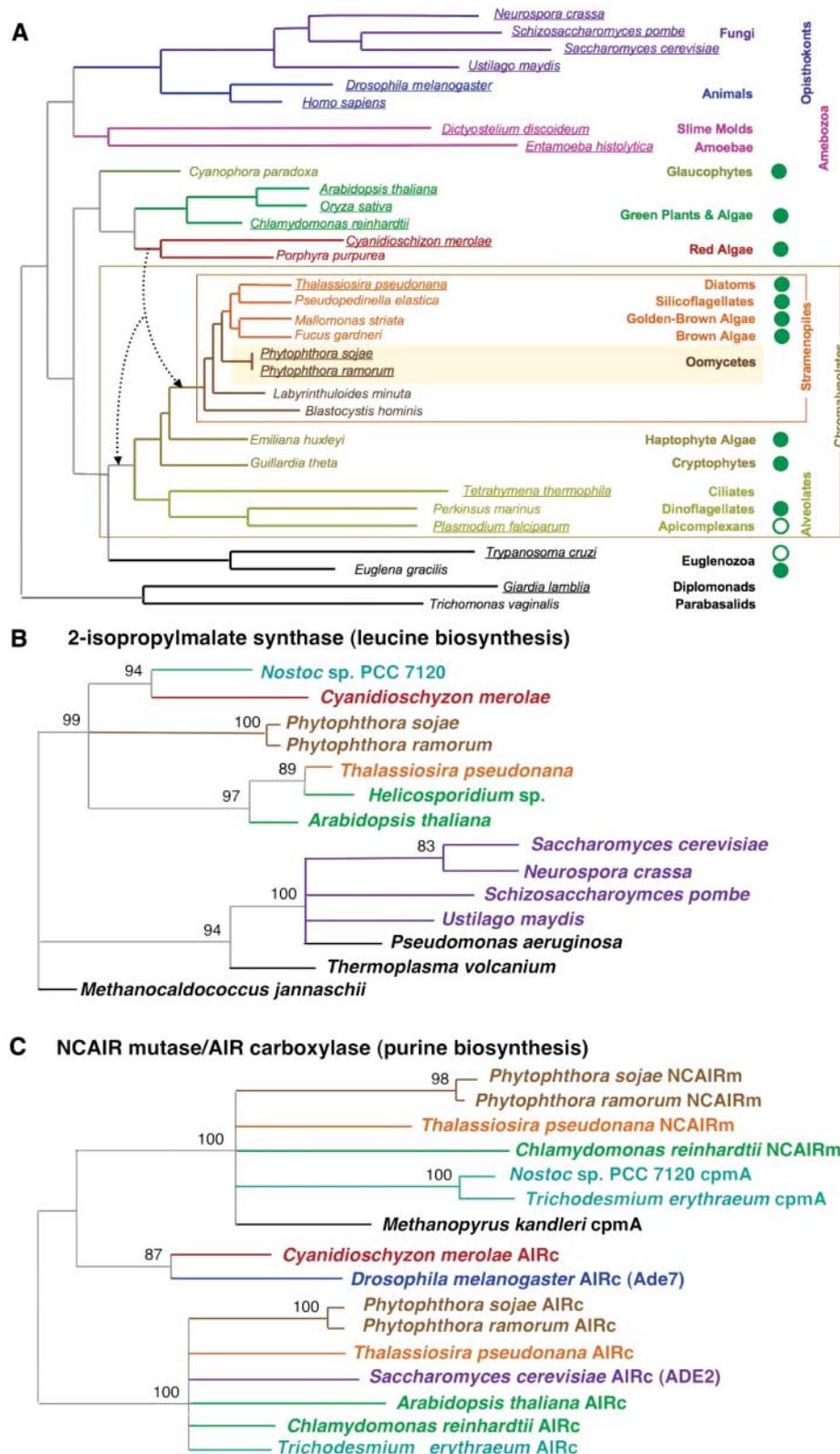
Fig. 1. Identification of genes potentially originating from a photosynthetic endosymbiont. (**A**) Schematic phylogenetic tree of the eukaryotes. The tree is adapted from that of Baldauf *et al*. (*5*) that is based on a concatenation of six highly conserved proteins. Filled green circles on the right indicate photosynthetic species, open green circles indicate species with vestigial plastids of photosynthetic origin. The dotted arrows indicate hypothetical events in which an ancient red algal endosymbiont might have been acquired by an ancestor of the chromalveolates (left arrow) or of the stramenopiles alone (right arrow). (**B** and **C**) Phylogenetic trees produced using maximum parsimony (with the branch and bound algorithm) of amino acid sequences with the computer program PAUP 4.0b10 (*32*). Inferred amino acid sequences were aligned using ClustalW, and these were manually trimmed at each end to a position of confident alignment. (B) and (C) show strict consensus trees for two and three equally parsimonious trees, respectively. In both cases, numerals indicate bootstrap support values, and any with less than 80% have been collapsed. Branch lengths are proportional to sequence change using the accelerated transformation mode for character state reconstruction. Trees were rooted by specifying *Methanocaldococcus jannaschii* and the NCAIR mutase/cpmA cluster of genes as outgroups for (B) and (C), respectively. Taxonomic affinities of the organisms listed are as in (A), with the following additions: green plants, *Helicosporidium* sp.; cyanobacteria, *Nostoc* sp., *Trichodesmium erythraeum*, and *Synechocystis* sp.; other eubacteria, *Pseudomonas aeruginosa*, *Bacillus halodurans*, and *Clostridium acetylbutylicum*; archaebacteria, *Thermoplasma volcanium*, *M. jannaschii*, and *Methanopyrus kandleri*. In (C), NCAIRm, AIRc, and cpmA denote, respectively, N-phosphoribosyl-carboxy-aminoimidazole (NCAIR) mutase, 1-(5-phosphoribosyl)-5-amino-4-imidazole (AIR) carboxylase, and the circadian modifer gene cpmA that is a member of the NCAIR mutase family (*14*).

Fig. 2. Long-range gene colinearity between the genomes of *P. sojae* and *P. ramorum*. In (**A**) and (**B**), black and red lines link orthologs of like and reversed orientation, respectively. In (**A**), colored bars indicate orthologs located in different *P. sojae* sequence scaffolds. Gray bars indicate genes without orthologs. Filled red circles indicate scaffolds linked by a single end-sequenced BAC, and open red circles indicate scaffolds linked by end-sequenced BAC contigs. The boxed area in (**A**) is enlarged in (**B**).
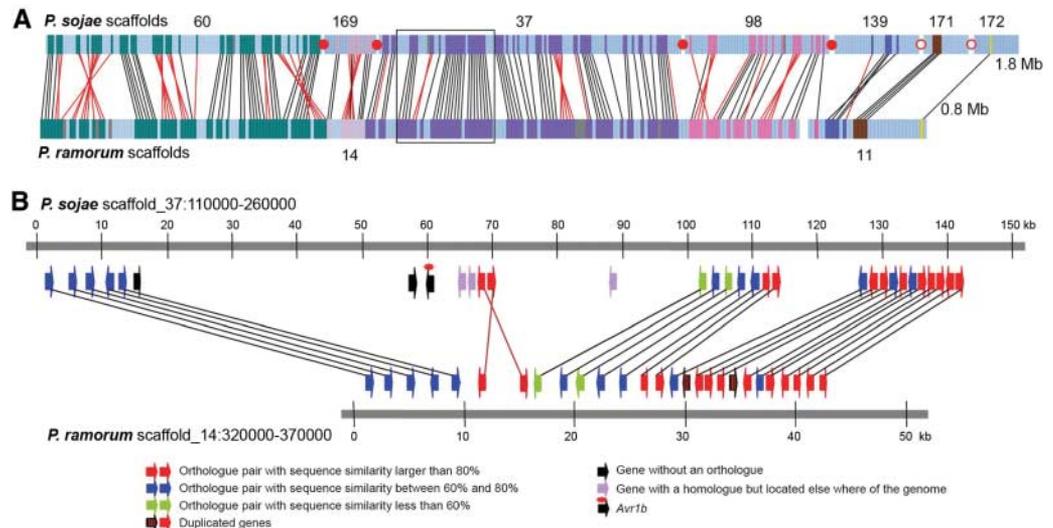
Fig. 3. Sequence divergence of two potential families of pathogenicity genes. (**A**) NPP1 or Nep1-like (NLP) protein sequences. A total of 89 sequences were used to construct this phylogram, including 40 *P. ramorum* and 29 *P. sojae* sequences. The remaining sequences were retrieved from GenBank. Protein sequences were edited to remove signal peptides and other domains and were aligned using ClustalW, and the unrooted phylogram was made using the neighbor-joining method (MEGA 3.1). The scale bar represents 10% weighted sequence divergence. Species of origin are abbreviated as follows: An, *Aspergillus nidulans*; Bh, *Bacillus halodurans*; Ec, *Erwinia caratovora*; Fo, *Fusarium oxysporum*; Gz, *Giberella zeae*; Mg, *Magnaporthe grisea*; Nc, *Neurospora crassa*; Pa, *Pythium aphanidermatum*; Pi, *Phytophthora infestans*; Pm, *Pythium monospermum*; Pp, *Phytophthora parasitica*; Ps, *Phytophthora sojae*; Pr, *Phytophthora ramorum*; Sc, *Streptomyces coelicolor*; Vd, *Verticillium dahlia*; Vp, *Vibrio pommerensis*. (**B**) Similarity of *P. sojae* Avh genes to *P. ramorum*. Purple indicates Avh genes, and crimson indicates a set of randomly chosen *P. sojae* genes having a functional annotation. The red arrow indicates the class that contains the *Avr1b*-1 gene itself.
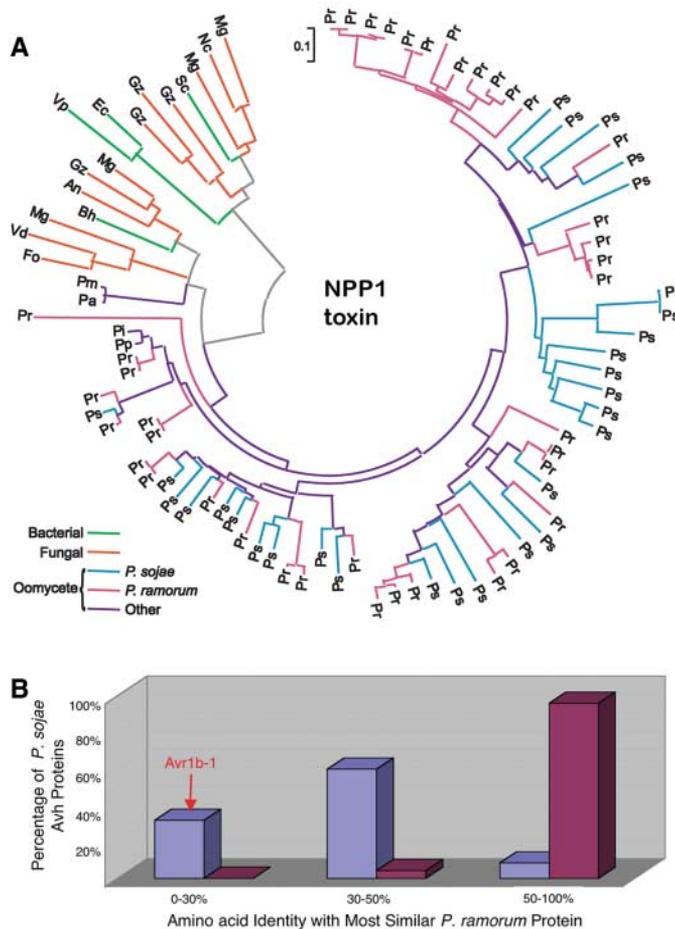
Because *P. sojae* and *P. ramorum* have very different host ranges, it is expected that some of their genes involved in host interactions will have rapidly diverged between the two

species as a result of strong selection for effective pathogenesis. Because *Phytophthora* species are cellular pathogens, secreted proteins are prime candidates for mediators of host

interactions (*18*). The predicted secretomes (*7*) of the two species (1464 and 1188 proteins, respectively) are evolving significantly more rapidly than the overall proteome. For example, 17% and 11% of the secreted *P. sojae* and *P. ramorum* proteins, respectively, are unique at the 30% identify level, whereas only 9% and 4%, respectively, of the overall proteomes are unique. The relatively rapid diversification of the secretomes is also evident in the number of multigene families encoding these proteins: 77% of the proteins belong to families of two or more members, and 30% belong to families of 10 or more members.

Both *P. sojae* and *P. ramorum* derive their nutrition biotrophically from living plant tissue during the initial hours of infection, but they switch to necrotrophic growth once the infection has been established, deriving their nutrition from killed plant tissue. As hemibiotrophs, the two species are expected to produce gene products that enable them to evade or suppress the plant's defense responses during early biotrophic infection and to produce gene products that kill and destroy plant tissue during later necrotrophic growth. Table 1 summarizes a wide variety of hydrolytic enzymes encoded by the genomes of the two species in comparison with the genome of the diatom *Thalassiosira pseudonana*, an autotroph. These destructive enzymes potentially could be associated with the necrotrophic phase. The two *Phytophthora* genomes encode large numbers of secreted proteases in contrast to the diatom and also encode the pectinases and cutinases required for hydrolyzing plant cell wall and cuticular material. The number of proteinase inhibitor genes required to protect the pathogens from plant proteases is also expanded in the *Phytophthora* genomes.

Gene families encoding proteins previously demonstrated to be toxic to plants show striking diversification; fewer than 25% of the genes remain identifiably orthologous between the two

Table 1. Potential infection-related genes in the *P. sojae* and *P. ramorum* genome sequences.

Gene product	Numbers of genes			
	P. sojae	*P. ramorum*	Orthologs*	Diatom
Hydrolases				
Proteases, all	282	311	221	314
Extracellular	47	48	38	8
Serine proteases	119	127	86	123
Metalloproteases	71	86	62	84
Cysteine proteases	67	74	52	63
Glycosyl hydrolases	125	114	54	n.d.†
Secreted	56	37	23	n.d.
Pectinases				
Pectinesterases	19	15	n.d.	0
Pectate lyases	43	41	n.d.	0
Cutinases	16	4	1	0
Chitinases	5	2	2	49
Lipases	171	154	n.d.	n.d.
Phospholipases	>50	>50	n.d.	23
Phospholipase C	0	0	0	3
Phospholipase D	18	18	18	3
Protease inhibitors, all	22	19	13	9
Kazal	15	12	8	2
Cystatin	4	4	4	0
Protein toxins				
NPP family‡	29	40	7	0
PcF family§				
Six Cys family	2	4	0	0
Eight Cys family	17	0	0	0
Crn family‖	40	8	2	0
Secondary metabolite biosynthesis				
Nonribosomal peptide synthetases	4	4	4	16
Polyketide synthases	0	0	0	0
Cytochrome P450's	30	24	21	10
CYP51 clan	0	0	0	1
ABC transporters	134	135	105	63
PDR¶ (ABCG-full)	45	46	30	3
ABCG-half	23	22	19	6
MDR# (ABCB)	7	7	4	3
MRP** (ABCC)	23	22	19	6
Effectors				
Elicitins	18	17	13	0
Elicitin-like	39	31	22	0
Avh (RXLR) family	350	350	83 (21)††	0

*Genes orthologous between *P. sojae* and *P. ramorum* were estimated based on bidirectional best BLAST hits and/or using similarity trees created by ClustalW. †n.d., not determined ‡Necrosis and ethylene-inducing protein family (19, 20). §(18, 21). ‖Crinkling and necrosis-inducing protein family (22). ¶Pleiotropic drug resistance transporters. #Multi-drug resistance transporters. **Multi-drug resistance–associated transporters. ††For the Avh family, the estimations of orthology are uncertain due to the rapid divergence of this family. The number in parentheses refers to orthologs that are syntenic and hence most likely to be correct.

species, and in several cases there are no identifiable orthologs (Table 1). There are also substantial differences in sizes of the gene families. The NPP1 family (19, 20) is more expanded and diversified in *P. ramorum*, whereas the PcF (18, 21) and crn (22) toxin families are more expanded in *P. sojae*. Figure 3A illustrates the explosive diversification of the NPP1 toxin family in the genus *Phytophthora*. This toxin family is interesting because several fungal plant pathogens also contain NPP1 toxin genes (19, 20), but they contain only two to four genes, whereas the *Phytophthora* species contain 29 or 40 (Fig. 3A).

The largest and most diverse family of infection-associated genes identified in the *P. sojae* and *P. ramorum* genomes is a superfamily with ~350 genes in each genome (7) that are similar to four oömycete genes identified as "avirulence" or "effector" genes, namely *Avr1b*-1 of *P. sojae* (8), *Avr3a* of *P. infestans* (23), and *Atr*1 (24) and *Atr*13 (25) of *Hyaloperonospora parasitica*. We have termed these Avh (avirulence homolog) genes. Avirulence genes were historically identified by their genetic interaction with plant disease resistance genes that encode defense receptors (26). In bacterial plant pathogens, some avirulence proteins function to

promote infection by suppressing the plant defense response—hence their renaming as "effector" proteins (26). Many of these bacterial effector proteins are injected into host cells by the type III secretion machinery (26), which explains the intracellular location of many resistance gene–encoded plant defense receptors. Intriguingly, the plant defense receptors that interact with the four cloned oömycete avirulence proteins also have a predicted intracellular location (8, 23–25, 27). However, the mechanisms by which the oömycete proteins may enter the plant cell are unknown. The four oömycete avirulence proteins share only very modest sequence similarity, but they do share two motifs, named RXLR and dEER, near the N terminus (24, 28) which are also shared by all of the 700 Avh gene products. Comparison of the 700 Avh sequences reveals a nonrandom distribution of amino acid residues surrounding each motif (7), which could potentially contribute to the their functions. Similarity of the RXLR motif to a motif used by the malaria parasite to transport proteins across the membrane of the parasitiphorous vacuole into the cytoplasm of human erythrocytes (29, 30) suggests that the RXLR motif may function to transport oömycete effector proteins into the plant cytoplasm. Figure 3B shows that the Avh gene family has undergone extensive diversification in comparison with a random set of *P. sojae* and *P. ramorum* genes. The diversification of the Avh family, driven presumably by selection pressure from the host defense machinery, underlines the potential importance of this superfamily for infection by these pathogens. Further characterization of these genomes will be published elsewhere (31).

References and Notes
1. D. C. Erwin, O. K. Ribiero, *Phytophthora Diseases Worldwide* (APS Press, St. Paul, MN, 1996).
2. D. M. Rizzo, M. Garbelotto, E. M. Hansen, *Annu. Rev. Phytopathol.* **43**, 309 (2005).
3. S. Kamoun, *Eukaryot. Cell* **2**, 191 (2003).
4. B. M. Tyler, *Trends Genet.* **17**, 611 (2001).
5. S. L. Baldauf, A. J. Roger, I. Wenk-Siefert, W. F. Doolittle, *Science* **290**, 972 (2000).
6. H. S. Yoon, J. D. Hackett, G. Pinto, D. Bhattacharya, *Proc. Natl. Acad. Sci. U.S.A.* **99**, 15507 (2002).
7. Materials and methods are available as supporting material on *Science* Online.
8. W. Shan, M. Cao, D. Leung, B. M. Tyler, *Mol. Plant Microbe Interact.* **17**, 394 (2004).
9. S. L. Kelly *et al.*, *Biochem. Soc. Trans.* **29**, 122 (2001).
10. M. J. Rebecchi, S. N. Pentyala, *Physiol. Rev.* **80**, 1291 (2000).
11. T. A. Randall *et al.*, *Mol. Plant Microbe Interact.* **18**, 229 (2005).
12. J. D. Hackett *et al.*, *Curr. Biol.* **14**, 213 (2004).
13. S. Li, T. Nosenko, J. D. Hackett, D. Bhattacharya, *Mol. Biol. Evol.* **23**, 663 (2006).
14. V. Dvornyk, *Microbiol.* **152**, 75 (2006).
15. P. F. Morris, E. W. B. Ward, *Physiol. Mol. Plant Pathol.* **40**, 17 (1992).
16. M. J. Caterina, P. N. Devreotes, *FASEB J.* **5**, 3078 (1991).
17. D. Bakthavatsalam, H. J. G. Meijer, A. A. Noegel, F. Govers, *Trends Microbiol.*, in press, doi: 10.1016/j.tim.2006.07.006.
18. S. Kamoun, *Annu. Rev. Phytopathol.* **44**, 41 (2006).

19. G. Fellbrich *et al.*, *Plant J.* **32**, 375 (2002).
20. D. Qutob, S. Kamoun, M. Gijzen, *Plant J.* **32**, 361 (2002).
21. G. Orsomando *et al.*, *J. Biol. Chem.* **276**, 21578 (2001).
22. T. A. Torto *et al.*, *Genome Res.* **13**, 1675 (2003).
23. M. R. Armstrong *et al.*, *Proc. Natl. Acad. Sci. U.S.A.* **102**, 7766 (2005).
24. A. P. Rehmany *et al.*, *Plant Cell* **17**, 1839 (2005).
25. R. L. Allen *et al.*, *Science* **306**, 1957 (2004).
26. J. H. Chang, A. K. Goel, S. R. Grant, J. L. Dangl, *Curr. Opin. Microbiol.* **7**, 11 (2004).
27. H. Gao, N. N. Narayanan, L. Ellison, M. K. Bhattacharyya, *Mol. Plant Microbe Interact.* **18**, 1035 (2005).
28. P. R. Birch, A. P. Rehmany, L. Pritchard, S. Kamoun, J. L. Beynon, *Trends Microbiol.* **14**, 8 (2006).
29. M. Marti, R. T. Good, M. Rug, E. Knuepfer, A. F. Cowman, *Science* **306**, 1930 (2004).
30. N. L. Hiller *et al.*, *Science* **306**, 1934 (2004).
31. A series of papers describing detailed analyses of the *P. sojae* and *P. ramorum* genome sequences will be published in a special issue of *Molecular Plant-Microbe Interactions* in December 2006.
32. D. Swofford, *PAUP*: Phylogenetic Analysis Using Parsimony* (and other methods)*, 4.0b7 beta version (Sinauer Associates Sunderland, MA, 2002).

REPORTS

Anomalous Spiral Motion of Steps Near Dislocations on Silicon Surfaces

J. B. Hannon,[1]* V. B. Shenoy,[2] K. W. Schwarz[1]

We have used low-energy electron microscopy to measure step motion on Si(111) and Si(001) near dislocations during growth and sublimation. Steps on Si(111) exhibit the classic rotating Archimedean spiral motion, as predicted by Burton, Cabrera, and Frank. Steps on Si(001), however, move in a strikingly different manner. The anomalous behavior can be understood in detail by considering how the local step velocity is affected by the nonuniform strain field arising from the dislocation. We show how the dynamic step-flow pattern is related to the dislocation slip system.

Dislocations strongly influence both the mechanical and electrical properties of solids, and have been investigated in detail for more than 50 years. Although most investigations have focused on bulk properties, dislocations also influence surface processes. Perhaps the most striking example is the realization by Frank (*1*) that dislocations mediate crystal growth under conditions of low supersaturation and provide the surface steps required to capture deposited atoms. On a low-index surface without dislocations, islands must spontaneously nucleate before such growth can occur.

More recently, there has been interest in exploiting the strain field of bulk dislocations to tailor surface properties. For example, periodic arrays of dislocations have been used to engineer the strain at the surface of a thin Si(001) film. The strain pattern can be used to preferentially nucleate Ge quantum dots at specific locations on a surface (*2*, *3*). Here, we describe how the dislocation strain fields influence step

motion during growth. By imaging the Si(001) surface in real-time at 1100°C, during growth and sublimation, we show that step motion near the dislocation core is inconsistent with classic models that predict rotating spiral step profiles (*4*). We find instead that the step velocity can be interpreted directly in terms of the surface strain field generated by a bulk dislocation.

Images of a step on Si(111) emerging from a screw dislocation (Fig. 1A) were obtained using low-energy electron microscopy (LEEM) (*5*) during sublimation at elevated temperatures ($T \approx 1100$°C). Si atoms evaporated from the terrace are replenished by atoms detaching from steps, causing the steps to retract. Burton, Cabrera, and Frank (BCF) (*4*) developed a simple theory of step motion near a dislocation
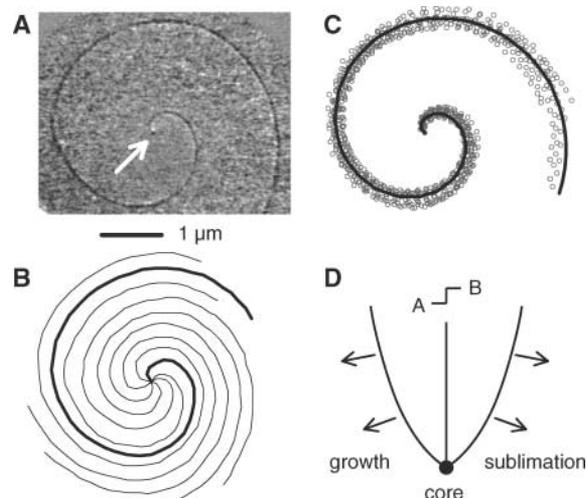

Fig. 1. (A to C) Step motion near a dislocation core on Si(111) during sublimation. (**A**) 40 eV LEEM image of a step emerging from a dislocation core measured at time t_1. The step curvature decreases monotonically away from the core (indicated by an arrow). (**B**) Position of the step at 5-s intervals as it winds (counterclockwise) about the core during sublimation. The curve corresponding to (A) is shown in bold. (**C**) Measured step profiles, each rotated by an angle $(t - t_1)/t_0$, where $t_0 = 36$ s is the period of the step motion and t is the time the profile was measured. The solid curve shows the prediction of the BCF model with $r_c = 93$ nm. (**D**) Spiral onset from growth and sublimation of a surface step emerging from a dislocation. The step separates two surface phases: A on the lower side of the step and B on the upper side. If the step direction is reversed, so is the direction of motion.

[1]IBM Research Division, T. J. Watson Research Center, Yorktown Heights, NY 10598, USA. [2]Division of Engineering, Brown University, Providence, RI 02912, USA.

*To whom correspondence should be addressed. E-mail: jbhannon@us.ibm.com